The 8th Pacific Rim International Congress on Advanced Materials and Processing
Edited by: Fernand Marquis
TMS (The Minerals, Metals & Materials Society), 2013

DETERMINATION OF FRACTURE TOUGHNESS VALUES OF TWO Ni – BASE SUPER ALLOYS FOR HIGH TEMPERATURE APPLICATIONS

Muhammad Hasibul Hasan[1], Mubarak AL-Grafi[2]

[1]International Islamic University Malaysia
P.O Box 10, 50728 Kuala Lumpur, Malaysia
[2]Taibah University,
P.O. Box 30064, Postal Code 41477 KSA

Keywords: Super alloys, fracture toughness, SEM

Abstract

Nickel-base Alloys 617 and 276 have been considered as structural material for turbine blades and nuclear hydrogen generation. The structural integrity of an engineering component is known to be influenced by the presence of surface irregularities such as cracks in the material. Hence Elastic plastic fracture mechanics base single compact tension specimen has been used to determine J_{1C} value for ductile crack growth behavior of austenitic Alloy 617 and 276 as a function of temperature. Alloy 617 showed fairly constant resistance to fracture from ambient temperature up to 500^0C for duplicate testing satisfying EPFM criteria. Whereas the J_{1C} values of alloy 276 were gradually reduced with increasing temperature, the reduction being more pronounced from ambient temperature to 100°C. Efforts have been made to calculate the values of K_{1C} and crack tip opening displacement for these alloys. Finally, fracture morphology in the loading and unloading sequences has been analyzed by SEM.

Introduction

1.1 Background
The cost of energy including conventional fossil fuels, such as oil and gas, has been increasing rapidly during this past decade. Among all other reasons, the increased cost is primarily due to the imbalance in supply and demand. In addition, the extensive use of fossil fuels has been receiving negative publicity in industrialized nations all over the world due to the generation of pollutant. In view of this rationale, the world is looking for alternative renewable energy sources. Wind energy is a renewable power source that produces no known significant atmospheric pollution. Currently the world wide capacity of installed wind energy stands at more than 40,000 MW with a 30% growth rate predicted over the next decade [1]. Alloy 617 and 276 were identified to be a suitable turbine blade material and heat-exchanger material for application in the gas turbine and Next Generation Nuclear Plant (NGNP) program [2]. Therefore, extensive metallurgical characterizations including the evaluation of tensile properties, fracture toughness, crack propagation rate and creep deformation of Alloy 617 and 276 at elevated temperatures were deemed necessary for their applications. This paper represents an essential part of the investigation, which was aimed at characterizing the metallurgical and mechanical behavior of candidate Alloy 617 and 276 in terms of fracture toughness for application in the wind turbine blade applications along with other conventional polister glass fiber materials.
Material Selection

High impact and abrasion blade material is recommended for the harsh environment like in sand storm prone desert area for the wind turbine. Wind speed and rotational speed of the blade determine impact velocity. Rotational speed is maximum at the outboard tip of airfoil, which is the furthest from the rotational axis of the wind turbine. The common technique for improving an airfoil's erosion resistance is to apply an elastometric material to the leading edge of the airfoil in the form of a tape. These tapes must be replaced frequently however, since they fail to adequately absorb the impact energy of the particulate matter. While polister-glass fiber blade materials encounter high impact erosion, nickel base super alloys could be candidates for these kinds of wind turbine applications because of their excellent tensile strength and superior corrosion resistance properties.

Ni-base Alloy 617 was developed during 1970's as an advanced sheet material for aerospace application. A combination of high strength and oxidation resistance at temperatures up to 1800°F (980°C) makes Alloy 617 a suitable material for ducting, combustion cans, and transition liners in both aircraft and land-based gas turbines. Both Alloy 617 and 276 have been used in catalyst-grid support for production of nitric acid, heat-treating baskets and reduction boats in the refining of molybdenum due to its high temperature corrosion resistance [3]. The literature data indicate that this alloy has been used in the fabrication of thermal energy storage capsules to contain eutectic fluoride mixtures of sodium, magnesium, lithium and potassium at temperatures of 1000K. Alloy 617 has also been used in the manufacture of retort furnace for the tritium extraction facility and high temperature gas cooled reactors. This material possesses excellent resistance to creep deformation and ruptures at temperatures up to 850^0C [4]. Further, it can maintain excellent metallurgical stability even after its long-term exposure at elevated temperatures. Relatively lower coefficient of thermal expansion of this alloy, compared to that of most austenitic stainless steels, enables Alloy 617 to be used in conjunction with ferritic steels. Also, its low density provides a high strength-to-weight ratio. Alloy 617 has also been considered by NASA as a candidate material for heat-shields in space transportation systems. This material can be strengthened by the precipitation of metal carbonitrides M(C,N) and homogeneously distributed $M_{23}C_6$ carbides resulting from a solution annealing treatment.

1.2 Scope

A mechanistic understanding of tensile deformation of Alloy 617 and 276 at temperatures ranging from ambient to 1000°C had already been presented by a previous investigator [5]. The structural integrity of metallic engineering components is known to be influenced by the presence of surface irregularities such as cracks. These metals/alloys may also be subjected to variable loading conditions due to fluctuating operating desert conditions and sand storms. Therefore, estimation of the fracture toughness of this alloy at different temperatures using elastic-plastic-fracture-mechanics (EPFM) concept [6] was calculated. Tested specimens were also investigated through scanning electron microscopy (SEM) to determine the morphology of failure.

Experimentation

2.1 Test Material

An experimental heat of Alloy 617 was custom-melted at the Huntington Alloys Corporation, West Virginia using a vacuum-induction-melting (VIM) practice. The VIM heat was subsequently processed into rectangular and round bars of different dimensions using forging and hot-rolling. The hot-rolled rectangular bars were subsequently subjected to cold-rolling operation to reduce their thickness. Since both round and rectangular bars had substantial residual stresses resulting from hot and cold-rolling operations, these processed materials were thermally treated to relieve these internal stresses. This thermal treatment consisted of solution-

annealing at 2150°F (1175°C) for variable time periods depending on the thickness of the processed bars. Such a thermal treatment is known to produce large-sized austenitic grains with annealing twins in Ni-base alloys. On the other hand, Alloy 276 was procured from a vendor in a properly heat-treated condition. This heat treatment consisted of solution-annealing of this alloy at 1163°C (2125°F) followed by rapid cooling, providing a fully austenitic microstructure The chemical composition and room temperature tensile properties of the as-received material are given in Tables 1 and 2, respectively.

Table 1. Chemical Composition of Alloy 617 (HV1160) and 276 (Z7437CG) (wt %)

Heat No.	C	Mn	Fe	S	Si	Cu	Cr	Ni	Al	Ti	Co	Mo
HV1160	0.06	0.121	0.002	0.009	0.004	0.001	22.10	54.80	0.87	0.29	12.17	9.52
Z7437CG	0.006	0.42	5.9	0.001	0.008	-	15.8	58.3	-	-	0.1	15.9

Table 2. Ambient-Temperature Tensile Properties

Heat No.	Yield strength, MPa	Ultimate tensile strength, MPa	%El	%RA	Hardness (R_B)
HV 1160	371	855	78.35	61.98	86.8
Z7437CG	354	794	87	60	79

2.2 Test Specimens

25.4 mm thick compact-tension (CT) specimen with a straight through notch was used to determine the fracture toughness (J_{1C}) of this alloy. The specimens were machined in such a way that the longitudinal rolling direction was normal to the crack plane. Both the specimen configuration and a pictorial view of the CT specimen are illustrated in Figure 1.

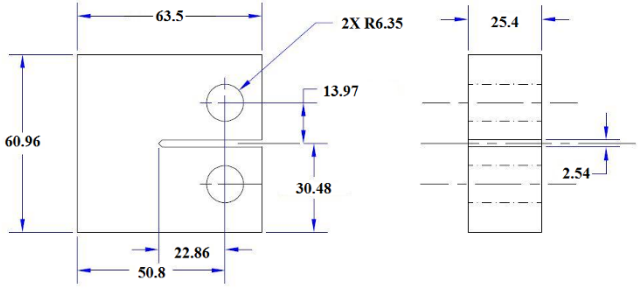

(a) Specimen Dimensions

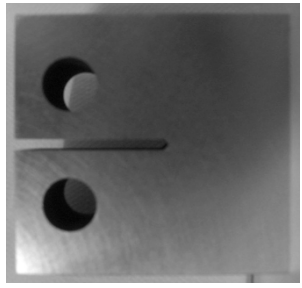

(b) Pictorial View
Figure 1. 25.4 mm CT Specimen

2.3 Test Procedure

At the outset, attempts were made to evaluate the fracture toughness of Alloy 617 and 276 in terms of plane strain fracture toughness (K_{1C}), based on the linear-elastic-fracture-mechanics (LEFM) concept [6]. However, the determination of K_{1C} is difficult from a practical point of view since CT specimens having unusually high thicknesses are needed to comply with the LEFM criterion [7]. Therefore, EPFM principle was used to evaluate the fracture toughness of this alloy in terms of J_{1C} according to the ASTM Designation E 813-1989 involving 25.4 mm thick CT specimens [8]. In essence, two types of J_{1C} testing method exist, namely single-specimen technique and multiple-specimen technique. The multiple-specimen technique requires at least five specimens [8] to be tested at a specific temperature to determine the J_{1C} value. Hence, to minimize cost and time, the single-specimen J_{1C} technique was used to determine the fracture toughness of Alloy 617 in this investigation with the help of Instron testing machine. Testing was conducted at temperatures ranging from ambient to 500°C. A 'J_{1C} Fracture Toughness' software [9], provided by the Instron Corporation was used to calculate and validate the J_{1C} value. The detailed procedure associated with the J_{1C} evaluation is described next.

Initially, the CT specimen was pre-cracked using the Instron machine to an approximate length of 3 mm [8] using an R value of 0.1 and a frequency of 1 Hz. The maximum load during pre-cracking was maintained at 20 kN [8]. It was then subjected to thirty loading and unloading sequences. Due to such loading/unloading sequences, the load-line-displacement (LLD) or, the crack-opening displacement (COD) i.e. the gap between the two arms of the specimens was increased. The LLD was measured by a high-temperature knife-edge extensometer, which was attached to the specimen arms at the beginning of the J_{1C} testing. The maximum travel of the extensometer was maintained at +/- 2 mm. A pictorial view of a typical J_{1C} test set-up including the extensometer is shown in Figure 2. A typical load versus LLD plot is shown in Figure 3 (a).

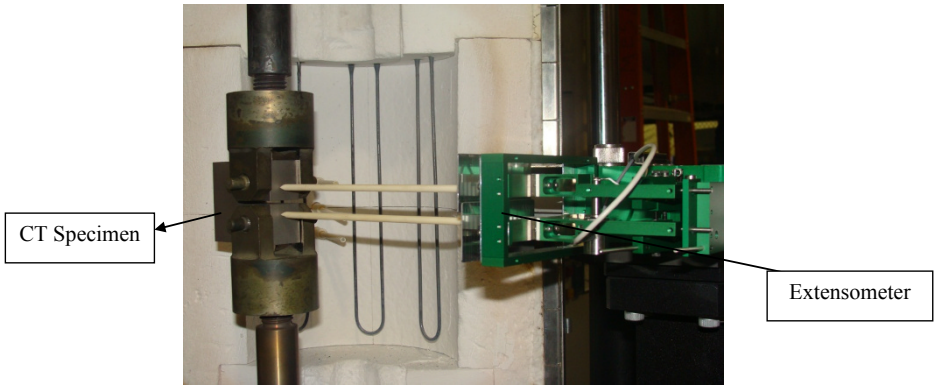

Figure 2. J_{1C} Test Set-up

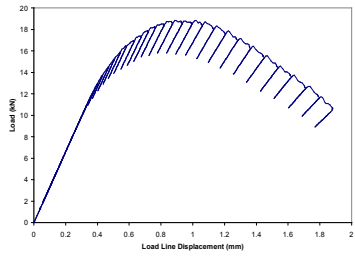

Figure 3 (a). Load versus LLD Plot

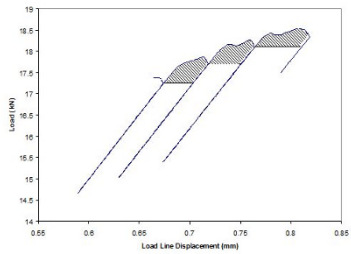

Figure 3 (b) Areas Representing J-Integral

The shaded area corresponding to each sequence, as shown in Figure 3 (b), represents the energy (J-Integral/J) needed to cause an increment of the crack length. The crack increases by a certain amount during each loading/unloading sequence. The J-Integral value for each area was calculated using Equations 1-3, given below [8, 10].

$$J = J_{elastic} + J_{plastic} \quad [1]$$

$$J_{elastic} = \frac{K^2}{E}\left[1 - \nu^2\right] \quad [2]$$

$$J_{plastic} = \frac{\eta_{pl}}{Bb}\int_0^{v_{pl}} Pdv_{pl} = \frac{\eta_{pl}}{Bb} \times A_{pl} \quad [3]$$

where

$$K = \text{Stress intensity factor, MPa}\sqrt{m} = \left[\frac{P}{\left(BB_N W\right)^{0.5}}\right] \times \alpha$$

P = Load, N

B = Specimen thickness, mm

B_N = Net specimen thickness, mm = B, in present study

W = Width of the CT specimen, mm

α = Geometric factor of the CT specimen
E = Elastic modulus of the material
ν = Poisson's ratio of the material, 0.3
b = Uncracked ligament, mm
$\eta_{pl} = 2 + 0.522b/W$
ν_{pl} = LLD / COD, mm
A_{pl} = Area corresponding to each loading / unloading sequence (mm^2)

Each J value, obtained by using Equations 1-3 was then plotted against the corresponding crack extension, as shown in Figure 4. The crack extension (a_i) for each sequence was measured by the unloading compliance principle, given by Equation 4 [8].

$$a_i/W = 1.000196 - 4.06319u_{LL} + 11.242u_{LL}^2 - 106.043u_{LL}^3 + 464.335u_{LL}^4 - 650.677u_{LL}^5 \quad [4]$$

where

$$u_{LL} = \frac{1}{\left[B_e E C_i\right]^{0.5} + 1}$$

B_e = Effective thickness of the CT specimen, mm = $[B - (B - B_N)^2/B] = B$ (since $B = B_N$), in current study
C_i = Specimen load line elastic compliance on an unloading/reloading sequence ($\Delta v/\Delta P$), mm/N
Δv = Increment in LLD/COD, mm
ΔP = Change in load, N

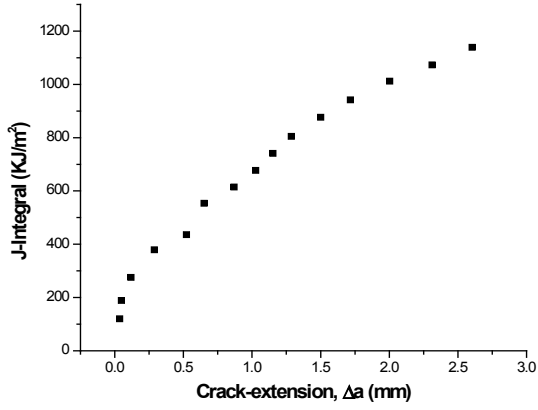

Figure 4. J-Integral vs. Crack-Extension

The data shown in Figure 4 was fitted to a power law curve and four different parallel lines were then drawn, as shown in Figure 5. These lines are referred to as the blunting line, 0.15-mm exclusion line, 1.5-mm exclusion line, and 0.2-mm exclusion line. These data are considered to be valid if at least one J-Δa point lies between the 0.15-mm extension line and a line parallel to the blunting line at an offset of 0.5-mm from the blunting line. The point of intersection of the power law curve and the 0.2-mm exclusion line (as shown in Figure 6) is usually taken as J_Q, or

the conditional J_{1C} value. J_Q is considered to be the J_{1C} value if the following two criteria are met:

- Thickness (B) of the specimen > [25 J_Q / σ_Y], where σ_Y = effective yield strength of the material = average of the yield and ultimate tensile strength (σ_{YS} and σ_{UTS}, respectively) of the material = [σ_{YS} + σ_{UTS}] / 2
- Initial uncracked ligament (b_0) > [25 J_Q / σ_Y]

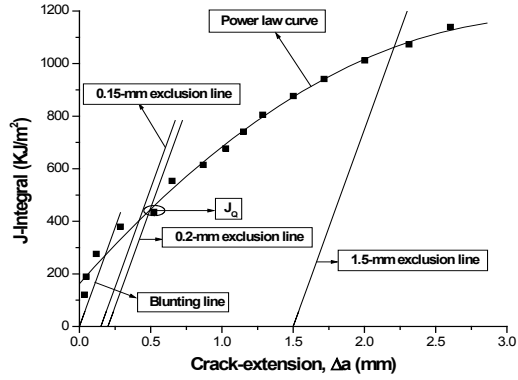

Figure 5. Determination of J_Q Using J-Integral versus Δa Plot

Efforts have also been made to correlate J_{1C} to K_{1C}. Literature [11,12] suggests that K_{1C} can be calculated from the J_{1C} value, according to Equation 5, as given below. Fracture toughness can also be measured using the crack-tip-opening-displacement (CTOD) method, which is based on Equation 6, given below [12].

$$K_{1C} = \sqrt{J_{1C} \times E / \left(1 - \nu^2\right)} \quad [5]$$

$$\delta = \frac{K_1^2}{mE\sigma_{YS}} \quad [6]$$

where
δ = CTOD, mm
$K_1 = K_{1C}$ value of the material, MPa$\sqrt{m}$
m = Constant = 2 for plane-strain condition
Further, tearing modulus has been calculated based on the flow stress and taking consideration of slopes of the J-integral vs. crack extension curves.

$$\sigma_f = \frac{1}{2}\left(\sigma_y + \sigma_{UTS}\right) \quad [7]$$

$$T = \frac{E}{\sigma_f^2} \cdot \frac{dJ}{da} \quad [8]$$

Where,

σ_f = Flow strength

σ_y = Yield strength

σ_{UTS} = Ultimate tensile strength

E = Young's modulus

$\frac{dJ}{da}$ = Slope of the J-integral vs. crack extension curve

Results

3.1 J_{1C} values

The measured J_Q values obtained from J_{1C} testing satisfied the validity criteria set by the ASTM Designation E 813-1989. The average J_{1C} values of Alloy 617and 276 tested at room temperature, 100, 200 and 500°C are superimposed in Figure 6. For alloy 617, data indicate that the J_{1C} values slightly decreased with increasing temperature, the reduction being more pronounced from room temperature to 100°C (118.6 to 114.1 kJ/m^2). From 200 to 500°C (109.88 to 109 kJ/m^2), the value of J_{1C} was almost constant. While for alloy 276 J_{1C} values gradually decreased with increasing temperature, the reduction being more pronounced from room temperature to 100°C (156 to 103 kJ/m^2). From 200 to 500°C (88 to 86 kJ/m^2), there was insignificant decrease in the J_{1C} value. A load versus LLD plot, and a J-Integral versus Δa plot used in J_{1C} calculation are illustrated in Figures 7 and 8, respectively.

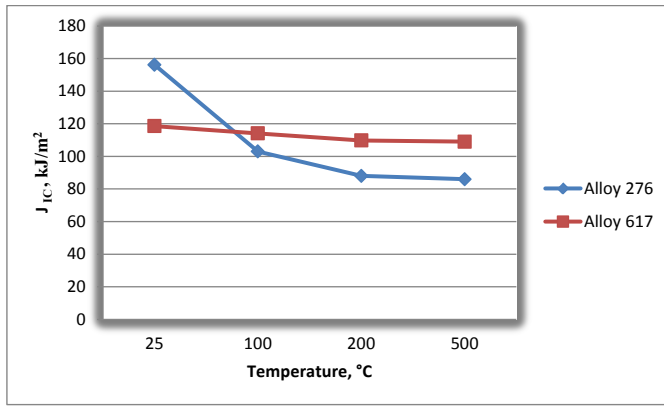

Figure 6. J_{1C} vs. Temperature

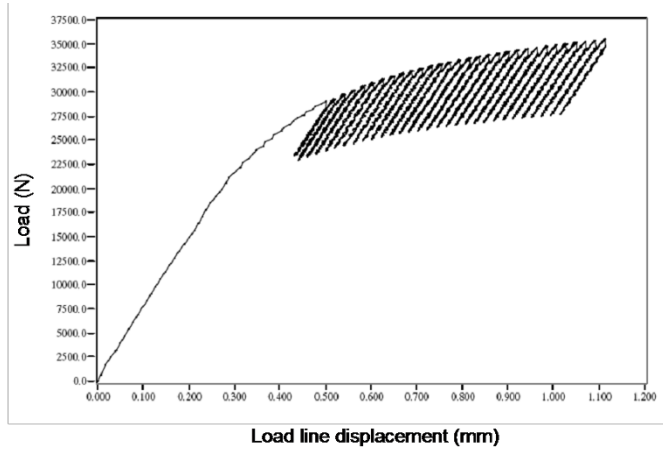

Figure 7. Load vs. LLD at Ambient Temperature

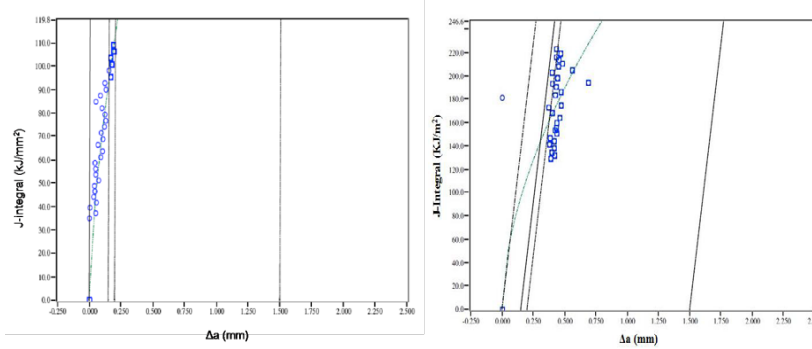

(a) Alloy 617 (b) Alloy 276

Figure 8. J-Integral vs. Δa at Ambient Temperature

3.2 Equivalent K_{1C} and CTOD values

The equivalent K_{1C}, and the CTOD values are given in Table 3. These values of fracture toughness of Alloy 617 and 276 closely match with the open literatures. Further, the calculated δ values for alloy 617 were very close to a range in CTOD values (0.1 to 0.2) for an adequately tough material [13]

Table 3. K_{1C} and δ Values vs. Temperature

Temperature (°C)	Alloy 617		Alloy 276	
	K_{1C} (MPa√m)	δ (mm)	K_{1C} (MPa√m)	δ (mm)
Room Temperature	163.05	0.175	186.8	0.24
100	159.53	0.204	151.9	0.19
200	156.94	0.213	140.5	0.18
500	156.34	0.245	139.0	0.22

3.3 Tearing modulus values

The tearing modulus is shown in semi-logarithmic scale as a function of temperature. Young's modulus of Alloy 617 has been determined by ASTM designation E 8-01 [14]. The respective flow stress has been calculated by taking average value of yield and ultimate tensile strength. Thus, the flow stress inherits the largest uncertainty in these considerations. Nevertheless, the tearing modulus follows the temperature dependency like the J-value. Literature suggests [15] large tearing moduli are to be seen in correlation with large stretch zones. As the investigation was limited up to 500^0C due to furnace setback, the tearing modulus remained fairly close within these temperature regimes. Once again, these values are excellent match with literature [15]

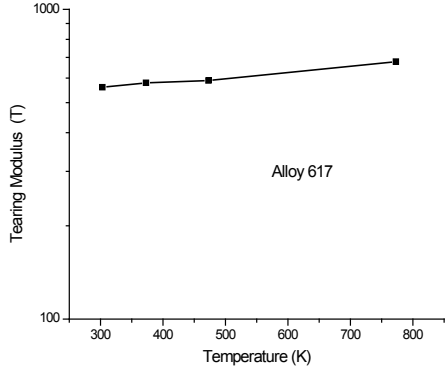

Figure 8. J-Integral vs. Δa at Ambient Temperature

3.4 Fractographic evaluations

The SEM micrographs of the tested CT specimens at room temperature are shown in Figure 9. These micrographs revealed three distinct regions, namely striations due to fatigue pre-cracking,

very prominent striations due loading/unloading sequences and finally dimple due to fast fracture.

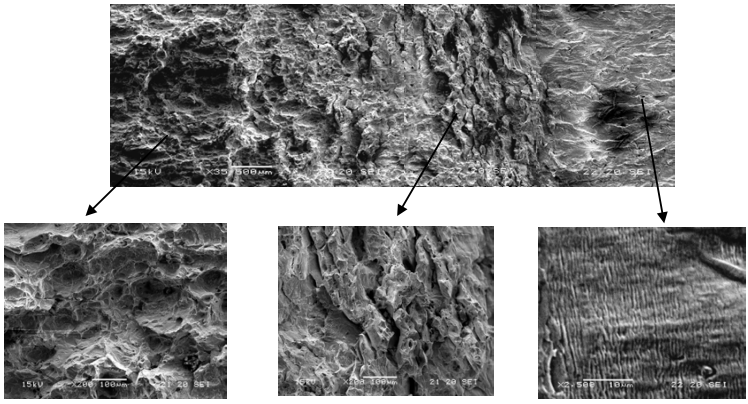

Fast Fracture, Dimples | 30 loading-unloading sequence | Pre cracking, Striations

Figure 9. SEM micrographs of tested specimens for Alloy 617

Conclusions

This study was focused on the evaluation of the fracture toughness behavior of the candidate structural materials for turbine blade, Alloy 617 and 276. The key results obtained from this investigation are summarized below.

- The J_{1C} values satisfied the validity requirements prescribed by the ASTM Designation E 813-1989.
- The effect of temperature on J_{1C} value for Alloy 617 is not that much significant up to 500^0C. The reduction in the J_{1C} value from 200 to 500°C was minimal. Further, tearing modulus was changed insignificantly along with the temperature as expected.
- There was a sharp reduction in the J_{1C} value for Alloy 276 from ambient temperature to 100°C, followed by a gradual decrease to 200°C. The reduction in the J_{1C} value from 200 to 500°C was minimal.
- Fractographic evaluations for both of the broken CT specimens revealed striations and dimpled microstructures.

Acknowledgement

The authors would like to thank UNLV, The National Science, Technology and Innovation Plan (NSTIP) and KACST through their grant (ASTP-09) to support the research work.

References

1. N. Dalili, A.Edrisy and R. Carriveau " A review of surface engineering issues critical to wind turbine performance" Renewable and Sustainable energy reviews, 13 (2009) 428-438.
2. Paul M. Mathias and Lloyd C. Brown "Thermodynamics of the Sulfur-Iodine Cycle for Thermochemical Hydrogen Production" Japan March 2003, 68th Annual Meeting of the Society of Chemical Engineers, Japan The University of Tokyo
3. U. Bruch, D. Schumacher, P. Ennis, E. Heesen, "Tensile and Impact Properties of Candidate Alloys for High-Temperature Gas-Cooled Reactor Applications", Nuclear Technology, vol. 66, 1984, pp. 357-362
4. Y. Sakai, T. Tanabe, T. Suzuki, H. Yoshida, "Corrosion Behavior of Inconel 617 in a Simulated HTGR Helium", Transactions of National Research Institute for Metals, vol. 27, 1985, pp. 20-27
5. Ajit Roy, Muhammad H. Hasan, Joydeep Pal "Creep deformation of Nickel-base superalloys at different temperatures", (accepted for publication) Materials science and Engineering: A.
6. Vikram Marthandam, "Tensile Deformation, Toughness and Crack Propagation Studies of Alloy 617", Ph.D. Dissertation, Mechanical Engineering, April 10, 2008
7. Xiao Guang, Zu Han Lai, " Realization of single specimen analytical method of J_{1C} determination by using compact tension loading". Engineering Fracture Mechanics , Vol 34 No.5/6, pp 1013-1021, 1989
8. ASTM Designation E 399-1999. "Standard Test Method for Linear-Elastic Plane-Strain Fracture Toughness K_{1C} of Metallic Materials." American Society for Testing and Materials (ASTM) International
9. ASTM Designation E 813-1989. "Standard Test Method for J_{1C}, A Measure of Fracture Toughness." American Society for Testing and Materials (ASTM) International.
10. Instron Corp. Fast Track 2 - J_{1C} Unloading Compliance Software.
11. Structural Integrity Associates Inc. "Nonlinear Fracture Toughness Testing." Technical Paper.
12. Perez, J.E., Ipiñaa, Yawnyb, A.A., Stukeb, R. & Oliverb, C. Gonzalez. "Fracture Toughness in Metal Matrix Composites." *Materials Research* 3 (2000): 74-78.
13. Hertzberg, Richard W. *Deformation and Fracture Mechanics of Engineering Materials*. NY: John Wiley & Sons, 1996.
14. "CTOD Testing." May 25, 2009. <http://www.twi.co.uk/content/jk76.html>.
15. ASTM Designation E 8-2001. "Standard Test Method for Tension Testing of Metallic Materials"
16. K. Krompholz, E.D. Grosser & K.Ewert. "Determination of J-integral R-curve for Hastelloy X and Inconel 617 up to 1223 K using Potential Drop Technique"